

Analysing high resolution digital Mars images using machine learning

Gergacz M.^{1,2,3} Keresztfuri A.^{3,4}

¹ ELTE Institute of Physics, H-1117 Budapest, Pázmány Péter 1/A, Hungary

² Wigner RCP, H-1121 Budapest, Konkoly-Thege Miklós 29-33, Hungary

³ Konkoly Thege Miklós Astronomical Institute, Research Centre for Astronomy and Earth Sciences, H-1121 Budapest, Konkoly-Thege Miklós 15-16, Hungary

⁴ CSFK, MTA Centre of Excellence, H-1121 Budapest, Konkoly-Thege Miklós 15-17, Hungary

Abstract

The search for ephemeral liquid water on Mars is an ongoing activity. After the recession of the seasonal polar ice cap on Mars, small water ice patches may be left behind in shady places due to the low thermal conductivity of the Martian surface and atmosphere. During late spring and early summer, these patches may be exposed to direct sunlight and warm up rapidly enough for the liquid phase to emerge.

To see the spatial and temporal occurrence of such ice patches, optical images should be searched for and checked. Previously a manual image analysis was conducted on 110 images from the southern hemisphere, captured by the High Resolution Imaging Science Experiment (HiRISE) camera onboard the Mars Reconnaissance Orbiter space mission. Out of these, 37 images were identified with smaller ice patches, which were distinguishable by their brightness, colour and strong connection to local topographic shading.

In this study, a convolutional neural network (CNN) is applied to find further images with potential water ice patches in the latitude band between -40° and -60° , where the seasonal retreat of the polar ice cap happens. Previously analysed HiRISE images are used to train the model, each was split into hundreds of pieces, expanding the training dataset to 6240 images. A test run conducted on 38 new HiRISE images indicates that the program can generally recognise small bright patches, however further training might be needed for more precise predictions. Using a CNN model may make it realistic to analyse all available surface images, aiding us in selecting areas for further investigation.

1 Introduction

The aim of this work is to test the automated detection of surface ice patches on images of the Martian surface, using a convolutional neural network (CNN) by teaching the system using manually selected proper images.

Understanding the possibilities of ephemeral water occurring on the surface of Mars under present day conditions is a main interest in Mars research. As the seasonal polar ice caps recede, small ice patches may remain in shaded areas. During summer as they are met with direct sunlight, irradiance increases and if the temperature is to rise fast enough, the possibility of the liquid phase appearing for a short time occurs [1]. The appearance of such ice patches is studied in this work, using high resolution images taken by the High Resolution Imaging Science Experiment (HiRISE) camera on board of the Mars Reconnaissance Orbiter (MRO).

Due to the low thermal conductivity and inertia of the Martian surface and atmosphere [2, 3], it is possible that small ice patches [4] may remain on the surface subsequent to the retreat of the seasonal polar cap in places where they are shielded from the light, for example by slope angles or on the poleward side of shadowing surface features. Over time water ice in these protected areas may also be exposed to direct sunlight, and then the ice may warm rapidly - it is not yet known whether or not a liquid phase [4, 5] may then appear, which is an important question for chemical transformations and the potential for life [6, 7, 8].

If the liquid phase emerges, it might influence slow, low temperature chemical changes on Mars, especially if supported by subzero temperature microscopic liquid water like proposed for hydrogen-peroxide decomposition [9] or for sulphate formation [10]. Such locations might need focused analysis in the future by orbiters monitoring them, which requires specific information on their location, the time period in which ice is present there and a selection of the best ones among them regarding potential chemical changes.

2 Methods

During the work manually selected images were used to teach the system what type of surface features should be searched for.

2.1 The HiRISE camera

The MRO spacecraft has been orbiting Mars since 2006 with the HiRISE camera on board and had imaged about 4% of the surface as of 2021, with many locations imaged repeatedly. The high-resolution camera has a mirror telescope with a diameter of 0.5 metres, making it the largest one ever used around another planet. From an altitude of 300 kilometres it can achieve a pixel size of 30 centimetres, making it possible to survey the surface in great detail.

The overall image size is 6 kilometres (20 000 pixels) in width by a programmable image length of up to 60 kilometres (200 000 pixels). It captures images between 14-16 local time, and produces colour images in the central portion of the field of view in three wavelength bands: 400-600 nm (blue-green, B-G), 550-850 nm (red, R) and 800-1000 nm (near infrared, NIR).

2.2 Surveyed region and dataset

Previously a manual survey has been conducted on HiRISE images using the JMars software [11, 12]. The area of interest was the latitude band between -40° and -70° in the seasonal range of 140° - 200° solar longitude, when the seasonal polar icecap is receding in the southern hemisphere. These images were analysed by eye and the surface features were characterised based on scientific publication and personal knowledge gained during the work. These images were then categorised into groups with and without sufficient remnant ice patches.

As of 2022, out of the approximately 1400 available HiRISE images that met the selection criteria, 110 ones were analysed manually. Potential residual ice patches were identified on 37 images from this dataset, which were used to teach the system for identification of similar patches on a large number of HiRISE images.

2.3 Convolutional Neural Network (CNN)

So far the image analysis has been done manually by eye, which is quite a time consuming task given the size of the images. Therefore increasing the dataset and potentially analysing all the available images would be achievable using an automatized system, which is being attempted in this work.

CNNs are successful in image classification tasks, while also being able to efficiently process large datasets. They extract local patterns and features by applying convolutional layers. These layers consist of convolutional kernels which slide over the input scanning the image, and by convolving these with the input image, textures, edges and gradients are extracted. The convolutional layers put out a feature map, which represents the activation of each kernel at different spatial locations. By applying a nonlinear activation function to that, the learning process becomes nonlinear and the network becomes able to recognise more complex connections between the detected features.

After convolution, pooling operations are applied to reduce the spatial dimensions of the feature maps and summarises the information in a local area, thus improving computational efficiency and enabling the network to focus on the presence of a feature, rather than the exact position of it in the input image.

3 The neural network

In this work a smaller Xception network [13] is used to tackle the problem. This type of network, unlike traditional CNNs that use convolutional layers sequentially, uses depthwise separable convolution. This means that the convolution operation is separated into two main steps, thus reducing the operations required and increasing computational efficiency. The structure of the applied model can be seen in Figure 1.

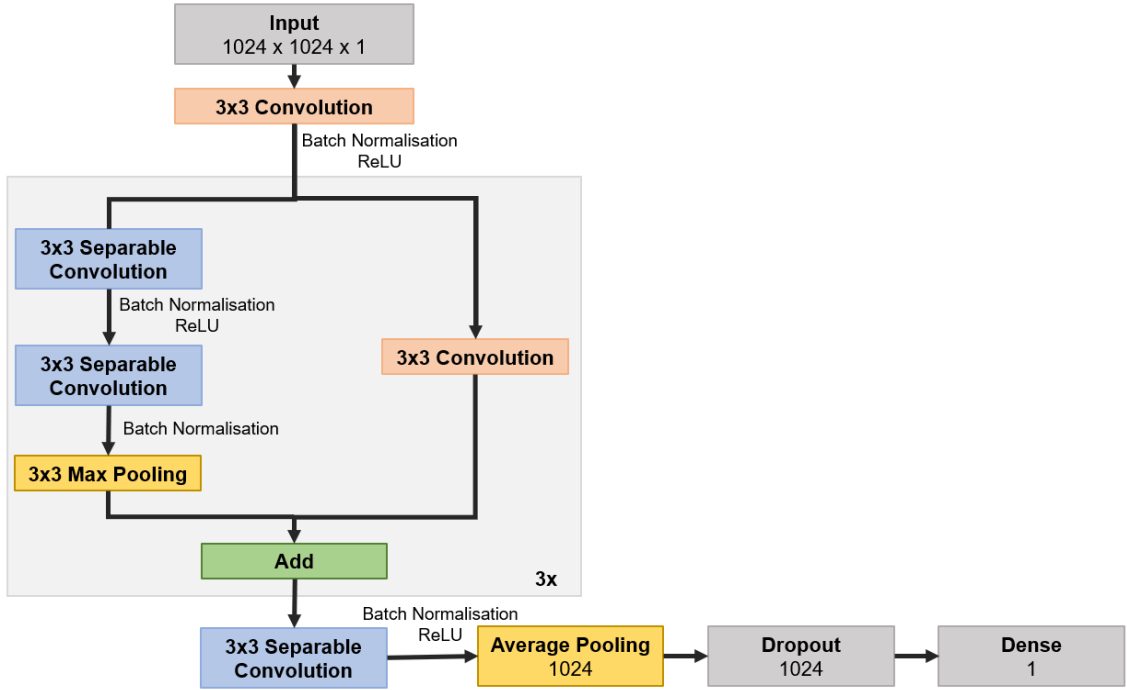


Figure 1. The structure of the model. Before each ReLU activation a Batch Normalisation is applied, to normalise the inputs to the activation and thus improve learning.

The model is running on a batch size of 25 through 25 training epochs. During one epoch the entire training dataset is processed by the network. After each epoch the parameters are updated and the network learns to make better predictions. However, using too many epochs is to be avoided as it can cause overfitting, which means that the network learns the noise too, it's not generalising well to new data. A 3x3 sized kernel is used with a stride of 2. The dropout rate is set to 0.5, ensuring that the model won't become overly reliant on specific nodes when making predictions.

The learning process of the network is supervised, meaning that the model is presented with labelled data during the training. The program's goal is to find patterns by which it can distinguish between data with different labels. Validation was conducted using 20% of the dataset on randomly selected samples. Since the network was trained to make a difference between two types of images, the final activation function was chosen to be a sigmoid function, as it is well suited for binary classification problems. For the same reason the loss

function is set for binary crossentropy function, which is typically paired with sigmoid activation functions. Optimization was conducted by the Adam optimizer [14]. This code was made with Keras with Tensorflow backend [15, 16], implemented in Python, while the training and testing was conducted on a processing unit provided by the Wigner Scientific Computing Laboratory.

4 Training dataset

In this study, there are two types of images we aim to distinguish between: images with small ice patches on them, and images that show none. To achieve this, HiRISE images were collected and organised in these two groups, which the program learned to distinguish between .

Given the size of the HiRISE images, they need to be chunked before loaded as input. This was done using the Mars Orbital Data Explorer Access software [17] which conducted the download from the Mars Orbital Data Explorer (ODE) site [18], the chunking process and deleted the chunks with black pixels around the centre of the image, leaving the black borders and majority of damaged pictures out of consideration. The uniform chunk size is 1024 pixel by 1024 pixel, which is a necessary size for the surface features to be taken into consideration during the training process, not just the bright patches themselves. The images were also converted to grayscale before chunking to improve training time. Another important aspect was that only a small portion of the Martian surface is imaged in HiRISE RGB, so it's crucial for the program to recognise ice patches in black and white.

Out of the analysed 110 HiRISE images 34 were picked out for training, 26 with small icy patches on them and 9 with none or with visible CO₂ sublimation on the surface (which were not interesting for this research as being too low temperature ice patches). After the chunking process the dataset is expanded to 6492 images, which is sufficient for training a CNN. The chunks from the 26 icy images were then individually categorised into icy and not icy chunks to make sure the data is organised properly.

A bright patch is considered icy, if it is located on the poleward side of a shadowing landform, does not cast shadow and has slightly diffuse edges. Identification was easier when the given bright spot was previously categorised as icy in RGB. These were considered as selection criteria for the automated evaluation of image chunks. 252 chunks with bright patches that were difficult to identify were left out of the training process.

After chunking and categorising, the dataset of 34 images was expanded to **6240 image chunks**. Out of these, 42% showed small ice patches visible, while the remaining chunks showed no ice patch or CO₂ sublimation was visible on the surface. Figure 2 is a visualisation of a small portion of the dataset used for training.

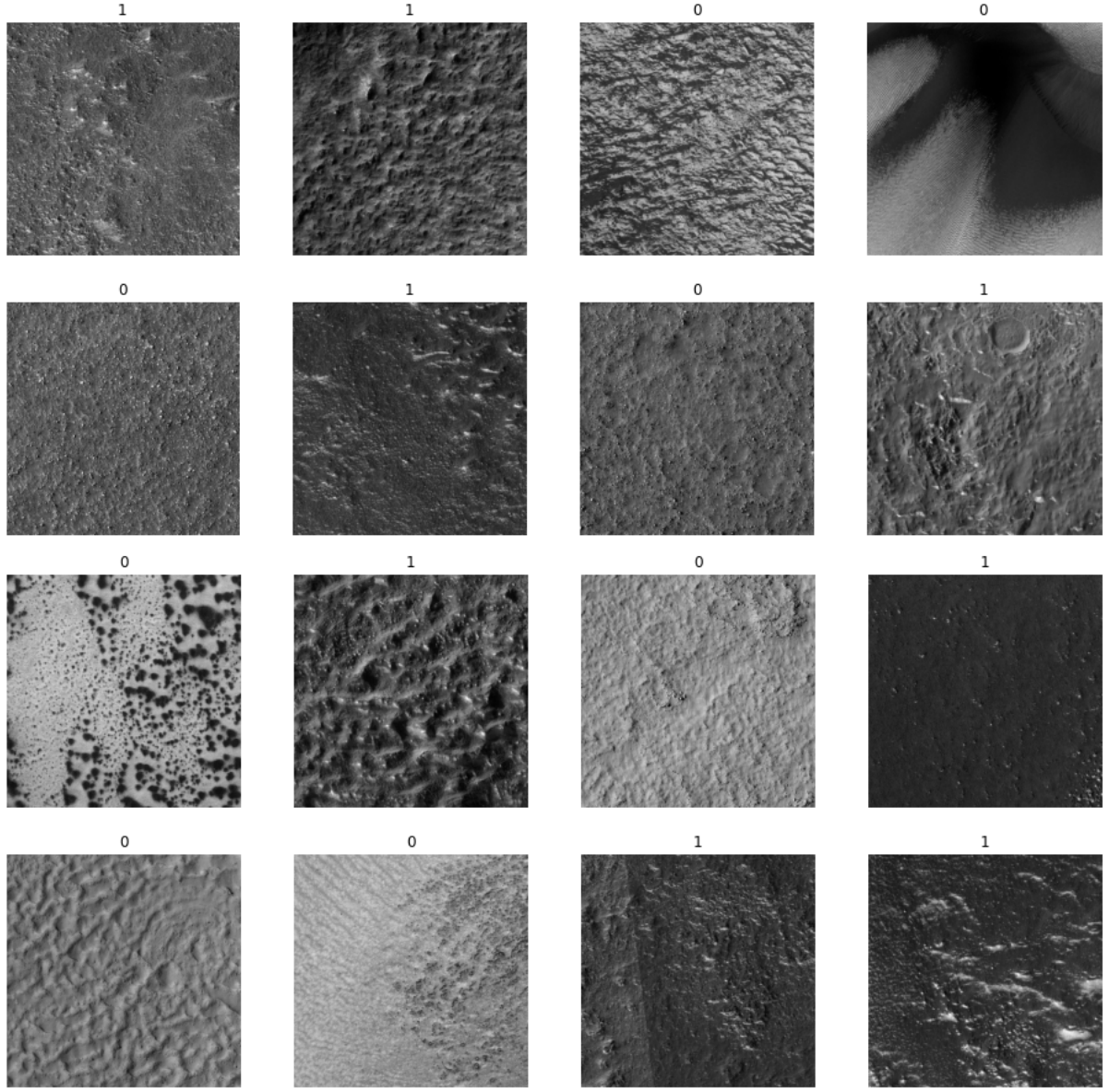


Figure 2: A few examples from the dataset. Images marked with 1 show small ice patches, while the ones with 0 have no small ice patch visible or CO_2 ice is sublimating from an extended area of the surface causing dark and not bright patches.

5 Results

This section has the following structure: discussing the loss and accuracy values, results of running the program on new data.

The evolution of the loss and accuracy values by the software during the epochs is shown in Figure 3. The **loss** measures the difference between the predicted output by the model and the true output, while **accuracy** measures the proportion of the correctly classified images by the model.

The gradual decrease of the loss along with the training epochs indicates that the model is improving in making better predictions over time. Occasional spikes in the curve can be

caused by the randomness introduced by dropout when a certain percentage (in this case 50%) of randomly selected nodes are dropped out, essentially removing the connections to and from these nodes. In the later epochs the curve can be seen to decrease more gradually, which indicates that further developments are difficult to achieve. As seen, the accuracy of the predictions increases as the loss decreases. By the last epoch, accuracy reached 98.08%. Validation was conducted using 1248 random images from the training dataset.

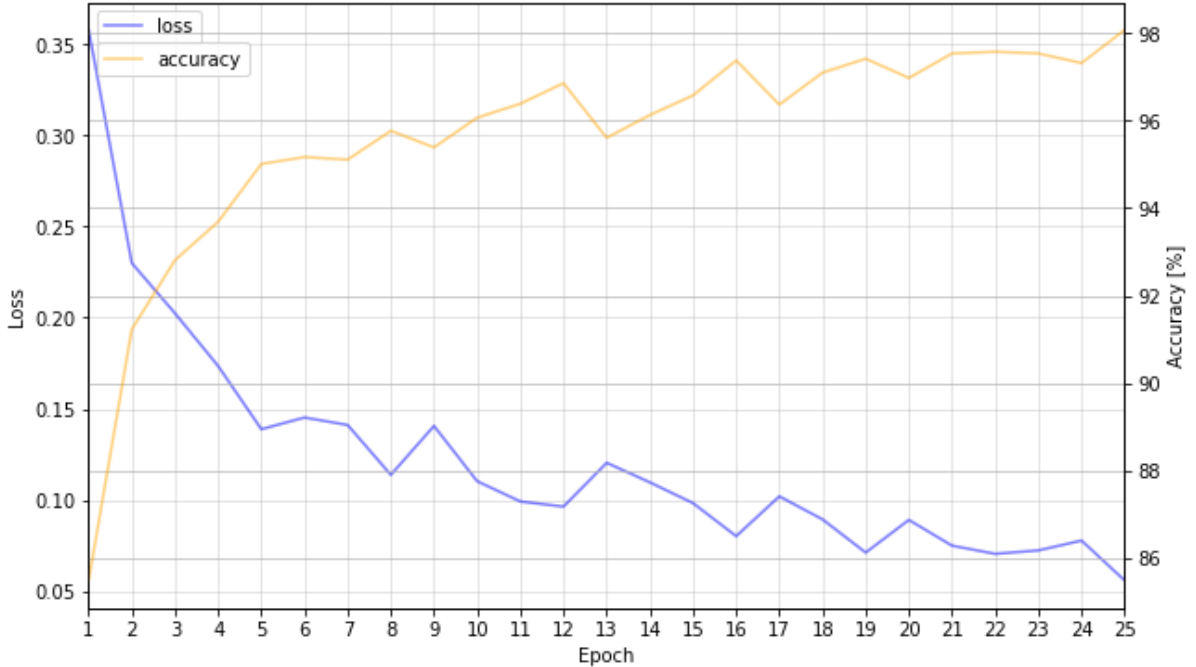


Figure 3: Evolution of the loss and accuracy during the training epochs. The decreasing trend of the loss indicates that the model is successfully learning to make better predictions.

The model analysed 38 new HiRISE images (cut into 13879 chunks) from the area and seasonal range of interest. Small insets of 307 m by 307 m sized areas are visualised in Figure 4 with their corresponding predictions for small ice patches present. Generally the program found the small icy patches, however it makes errors in some cases, like in image 3, 10, 17 and 18 for example. In these images bright spots are visible on the poleward side of shadowing forms, do not cast shadows and have diffuse edges, yet they were classified as images without small ice patches. In the case of 17 and 18 the error might come from the fact that there is only a slight difference in the tone of the shade between the surface and the bright patches, making identification difficult even during manual classification. Another error was made with image 7, where the model predicted a high probability for small ice patches. After manually analysing the image however, it became clear that the bright patches are mostly located in the sunlit parts of the landforms, e.g. they might be bright dust deposits. While bright patches can be observed on the poleward side as well, they are presumably made of the same material as the ones in sunlit areas.

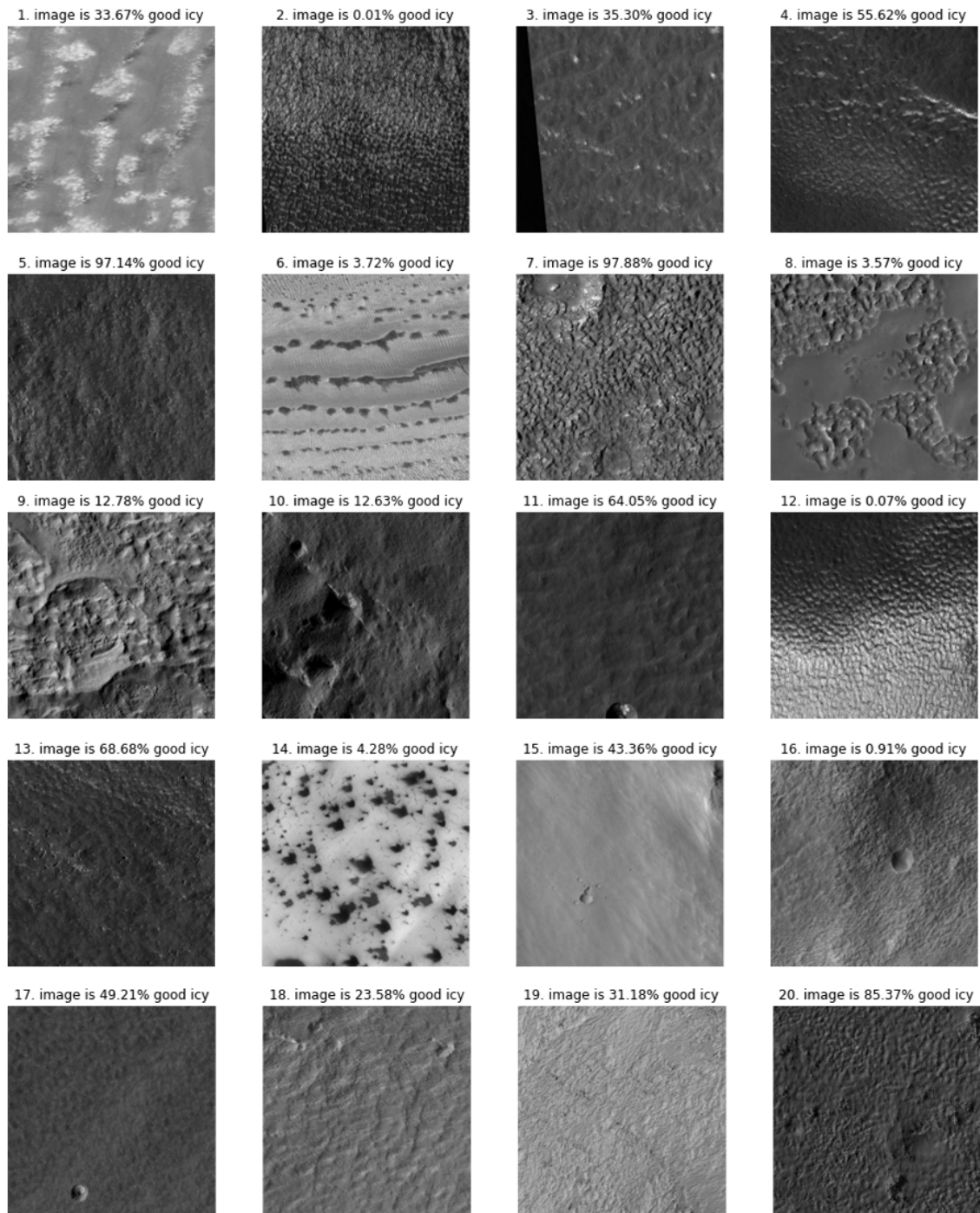


Figure 4: A few images and their corresponding predicted probability for having small icy patches visible. Above each image the predicted probability of them having small ice patches on the surface is displayed in a percentage. The model was successful in finding residual ice patches on image 4, 5, 11, 13 and 20, these were confirmed by manual analysis as well. On the other hand, the probabilities for image 3, 10, 17, 18 and 19 are not correct, as based on manual analysis they do have small ice patches present.

6 Summary

Out of the 38 HiRISE images, 16 were predicted to have no chunks with small icy patches, 15 to have more than 1 chunk with a higher predicted possibility than 60% to have small ice patches on them, and 9 to have only 1 such chunk. The prediction was manually checked for all HiRISE images and for 50 chunks out of the 13879 ones from the testing dataset.

The model's accuracy was 100% regarding the 16 HiRISE images that were predicted to have a low possibility of showing remnant ice patches, as after manually analysing them they were all classified as images with no small ice patch present. However, only 3 HiRISE images showed small icy patches out of the 15 that were predicted to have several such patches, and none out of the 9 with one predicted icy chunk.

The main reason for the low accuracy (13.6%) is that images with minor pixel anomalies (absolute bright pixels in the image that can be the result of errors during image processing or data transmission etc.) were not taken into consideration during the training. During the testing the model falsely identified these white pixels as ice patches in 5 HiRISE images and in more than 150 chunks. Further errors were commonly made by the model when a bright patch was located in the edge of the chunk, essentially cutting it in half in most cases. Bright patches located not only in shaded but in sunlit areas caused unreliable predictions too, as well as the low contrast between the surface and the brighter patch (image 15).

The program worked well with predicting the presence or absence in commonly occurring surface forms like stone fields, smaller craters (like in image 11 and 13) and polygonal cracks (like in image 5). These are the most common shading forms where ice remains after the seasonal recession of the polar ice cap, therefore most of the training dataset consisted of images with such shadowing features in them. More precise predictions can be achieved by running more training epochs, as on Figure 3 by the 25. training epoch the accuracy was still improving. Increasing the training dataset and introducing images with minor errors and more types of landforms may also aid the model in making less mistakes.

The model presented high accuracy predictions in recognising HiRISE images with no small ice patches present. Therefore using the program in the search for residual water ice patches may be beneficial, as it significantly decreases the number of HiRISE images that need to be analysed manually.

Acknowledgement

The authors thank the Wigner Scientific Computing Laboratory for their support and insightful discussions with the members.

References

[1] N. Schorghofer 2020. Crocus melting behind boulders on Mars. *The Astrophysical Journal* 890, 49. <https://doi.org/10.3847/1538-4357/ab612f>

[2] Grott M., et al. 2021. Thermal Conductivity of the Martian Soil at the InSight Landing Site From HP³ Active Heating Experiments. *JGR Planets* 126. <https://doi.org/10.1029/2021JE006861>

[3] Keresztfuri A., et al. 2011. Geologic field work on Mars: distance and time issues during surface exploration. *Acta Astronautica* 68, 1686-1701. <https://doi.org/10.1016/j.actaastro.2010.11.008>

[4] Langevin Y., et al. 2009. Investigations of selected areas of the south seasonal cap of Mars in early 2009

[5] Pál B., Keresztfuri A. 2017. Possibility of microscopic liquid water formation at landing sites on Mars and their observational potential. *Icarus* 282, 84–92. <https://doi.org/10.1016/j.icarus.2016.09.006>

[6] de Vera J., et al. 2014. Results on the survival of cryptobiotic cyanobacteria samples after exposure to Mars-like environmental conditions. *International Journal of Astrobiology* 13, 35-44. <https://www.doi.org/10.1017/S1473550413000323>

[7] Marschall M., et al. 2012. Migrating and UV screening subsurface zone on Mars as target for the analysis of photosynthetic life and astrobiology. *Planetary and Space Science* 72, 146-153. <https://doi.org/10.1016/j.pss.2012.05.019>

[8] Horváth A., et al. 2009. Analysis of Dark Albedo Features on a Southern Polar Dune Field of Mars. *Astrobiology* 9, 90-103.

[9] Keresztfuri A., Gobi S. 2014. Possibility of H₂O₂ decomposition in thin liquid films on Mars. *Planetary and Space Science* 103, 153-166. <https://doi.org/10.1016/j.pss.2014.07.017>

[10] Góbi S., Keresztfuri A. 2019. Analyzing the role of interfacial water on sulfate formation on present Mars. *Icarus* 322, 135-143. <https://doi.org/10.1016/j.icarus.2019.01.005>

[11] Gergácz M., Keresztfuri Á. 2022. Melting possibility of remnant seasonal water ice patches on Mars. [arXiv:2212.02166](https://arxiv.org/abs/2212.02166)

[12] Christensen et al. 2009. JMARS – A Planetary GIS

[13] F. Chollet et al. 2020. Image classification from scratch. https://keras.io/examples/vision/image_classification_from_scratch/

[14] D. P. Kingma and J. Ba, Adam: A method for stochastic optimization (2017), [arXiv:1412.6980 \[cs.LG\]](https://arxiv.org/abs/1412.6980) .

[15] F. Chollet et al. 2015. Keras. <https://keras.io>

[16] M. Abadi, et al. 2016. Tensorflow: Large-scale machine learning on heterogeneous distributed systems. [arXiv:1603.04467 \[cs.DC\]](https://arxiv.org/abs/1603.04467) .

[17] S. Sheriff 2019. Mars Orbital Data Explorer Access. <https://github.com/samiriff/mars-ode-data-access>

[18] J. Wang et al. 2019. PDS Geosciences Node’s Orbital Data Explorer of Mars Data Access. Ninth International Conference on Mars. 2019LPICo2089.6323W